JOURNAL OF NEUROTRAUMA 35:452–460 (February 1, 2018)

DOI: 10.1089/neu.2017.5174

Reduced Field of View Diffusion Tensor Imaging and Fiber Tractography of the Pediatric Cervical and Thoracic Spinal Cord Injury

Mahdi Alizadeh,[1] Joshua Fisher,[2] Sona Saksena,[2] Yusra Sultan,[3] Chris J. Conklin,[2] Devon M. Middleton,[2] Jürgen Finsterbusch,[4] Laura Krisa,[5] Adam E. Flanders,[2] Scott H. Faro,[6] M.J. Mulcahey,[7] and Feroze B. Mohamed[2]

Abstract

The aim of this study is to assess the utility and effectiveness of diffusion tensor imaging (DTI) and diffusion tensor tractography (DTT) of the entire pediatric cervical and thoracic spinal cord toward discrimination of typically developing (TD) controls and subjects with spinal cord injury (SCI). A total of 43 pediatric subjects, including 23 TD subjects ranging in age from 6 to 16 years old and 20 subjects with SCI ranging in age from 7 to 16 years, were recruited and scanned using a 3.0 Tesla magnetic resonance scanner. Reduced field of view diffusion tensor images were acquired axially to cover the entire spinal cord across two slabs. For DTI analysis, motion correction was performed by coregistration of the diffusion-weighted images to the reference image (b0). Streamline deterministic tractography results were generated from the preprocessed data. DTI and DTT parameters of the whole cord, including fractional anisotropy (FA), mean diffusivity (MD), tract length, and tract density, were calculated, averaged across the whole spinal cord, and compared between the TD and SCI groups. Statistically significant decreases have been shown in FA (TD = 0.46 ± 0.11; SCI = 0.37 ± 0.09; $p < 0.0001$) and tract density (TD = 405.93 ± 243.84; SCI = 268.90 ± 270.34; $p < 0.0001$). However, the mean length of tracts and MD did not show significant differences. When investigating differences in DTI and DTT parameters above and below the injury site, it was shown that the FA and tract density in patients with cervical SCI decreased significantly in the thoracic region. An identical trend was observed in the cervical region for patients with thoracic SCI as well. When comparing TD and SCI subjects, FA and tract density were the most sensitive parameters in detecting functional changes of the spinal cord in chronic pediatric SCI. The results show that both DTI and DTT have the potential to be imaging biomarkers in the diagnosis of SCI.

Keywords: diffusion tensor imaging; fiber tractography; pediatric; spinal cord injury

Introduction

After a traumatic or nontraumatic injury to the spinal cord, the affected individual will routinely undergo a series of evaluations to assess the condition of the cord and its functional abilities. To determine the clinical status of motor and sensory functions, clinicians typically use the International Standards for Neurological Classification of Spinal Cord Injury (ISNCSCI). The motor examination is completed through the testing of key muscle functions corresponding to the paired myotomes.[1] The sensory examination tests two aspects of sensation; light touch and sharp-dull discrimination in each of the 28 dermatomes on both sides of the body.[1] The severity of injury is classified by the American Spinal Injury Association (ASIA) Impairment Scale (AIS). This scale classifies the injury as complete or incomplete, with varying degrees of incomplete trauma depending on the presence motor or sensory function.[2,3]

In general, the outcomes of the ISNCSCI exam are valid when looking at adult spinal cord injury (SCI) cases. However, studies have shown that these examinations may not be applicable or accurate for the pediatric population. Therefore, additional examination techniques are required to diagnose pediatric SCI cases.[3]

A major shortcoming of the ISNCSCI is the absence of quantitative data that can be utilized in the diagnosis of pediatric SCIs.

Departments of [1]Neurosurgery and [2]Radiology, Jefferson Integrated Magnetic Resonance Imaging Center, Department of Radiology, Thomas Jefferson University, Philadelphia, Pennsylvania.
[3]Department of Biology, Drexel University, Philadelphia, Pennsylvania.
[4]Institut für Systemische Neurowissenschaften, Universitätsklinikum Hamburg-Eppendorf, Hamburg, Germany.
[5]Department of Physical Therapy, Thomas Jefferson University, Philadelphia, Pennsylvania.
[6]Department of Radiology, Johns Hopkins University, Baltimore, Maryland.
[7]Department of Occupational Therapy, Thomas Jefferson University, Philadelphia, Pennsylvania.

However, quantitative data can be obtained through magnetic resonance (MR) techniques such as diffusion tensor imaging (DTI) and diffusion tensor tractography (DTT). Spinal cord DTI is a method that tracks the diffusion of water molecules throughout the length of the cord.[4–7] The structure of the spinal cord can be differentiated into white matter (WM) and gray matter (GM). The WM consists of fibers that configure the ascending and descending tracts that carry information to or from the brain. The myelin sheath that insulates these tracts restricts perpendicular flow, resulting in diffusion that is predominantly longitudinal. Conversely, GM is not characterized by this organization of myelin and is therefore largely disordered, having a highly isotropic diffusion pattern. Thus, DTI can potentially help identify functional abnormalities by a more thorough characterization of the cord architecture.[4–10]

In the last decade, several reports have described the use of DTT to depict neuronal fibers in the WM of the brain. In contrast, high-resolution data for the spinal cord have been difficult to obtain, because of the small size of the spinal cord.[11] The spinal cord is located deeper in the body and surrounded with different types of tissue. Imaging the cord requires discriminating among tissues and materials with different magnetic properties, such as the spinal cord WM, GM, cerebral spinal fluid (CSF), vertebrae, muscle, and air, all of which are present within a small space.[11–15] These factors generally introduce susceptibility effects and reduce the amount of uncontaminated MR signal from the cord. Moreover, motion effects attributed to its proximity to the heart and lungs, particularly in the thoracic region of the cord, make imaging challenging in this region. Although it is difficult to obtain distortion-free, high-resolution images of the spinal cord using standard diffusion-weighted acquisitions, the implementation and optimization of a diffusion-sensitized two-dimensional (2D) radiofrequency (RF) reduced field of view (FOV) sequence allows for a higher in-plane resolution with fewer geometric distortions and physiologic based artifacts.[16] Also, the rigorous post-processing pipeline as implemented in this study is very critical and important for obtaining high-quality DTI and DTT results.[17]

As the performance of magnetic resonance imaging (MRI) improves, the number of DTI studies of the spinal cord has increased. There are two categories of such studies. One involves visualizing spinal cord disorders by tractography, including the visualization of inflammatory and degenerative disorders,[4–18] localization and characterization of spinal cord tumors,[13–19] characterization of the deformation, and interruption of local fibers caused by arteriovenous malformations,[20] Brown Sequard syndrome,[21] and SCI.[22,23] The other category involves the quantitative analysis and examination of correlations between diffusion and both functional and histological conditions.[7] DTI and DTT in pediatric subjects is limited to only a few studies,[2,22,24–26] and, to the best of our knowledge, there is no study reported with the investigation of DTT along the entire spinal cord (both cervical and thoracic) in subjects with SCI. The aim of this study is to assess the utility and effectiveness of DTI and DTT as imaging biomarkers for better discrimination of SCI for the entire pediatric cervical and thoracic spinal cord. To further this goal, DTI measurements above (in patient with thoracic SCI) and below (in patient with cervical SCI) the injury site were also investigated and compared to healthy control subjects.

Methods

Subject recruitment

A total of 43 pediatric subjects including 23 TD subjects between 6 and 17 years of age (11.94 ± 3.26 [mean ± standard deviation {SD}]; 13 females and 10 males) with no evidence of spinal cord pathology and 20 subjects with chronic SCI (10 subjects with cervical injury and 10 with thoracic injury) between 7 and 16 years of age (11.28 ± 3.00 [mean ± SD]; 9 females and 11 males) were recruited. Subjects and parents provided written assent and consent of the institutional review board approved protocol. The inclusion criteria used for subjects with SCI were: Subjects had stable SCI as evidenced by no neurological change in the past 3 months and were at least 6 months post-SCI. A range of the time after initial SCI is 1.4–17.0 years (7.33 ± 4.30). All subjects underwent a complete ISNCSCI examination on the same day as the MRI scan.[3] Severity of injury was determined according the AIS.[3] Of the subjects with SCI, there were 8 patients classified as AIS A (complete SCI), 2 with AIS B (sensory incomplete), and 6 with AIS D (sensory and motor incomplete). Unfortunately, 4 patients were unable to complete the ISNCSCI and therefore did not receive an AIS category because of age, low motivation, autonomic dysfunction, or lack of understanding of the instructions. Table 1 details the age at the time of study, age at the time of injury, time after initial SCI, and level and severity of injury for the SCI subjects.

Image acquisition

The MRI scans were performed using a 3.0 Tesla Siemens Verio MR scanner (Siemens Healthcare, Erlangen, Germany) with four-channel neck matrix and eight-channel spine array. 2D RF reduced FOV diffusion tensor images were collected axially in the same anatomical location prescribed for the T2-weighted images to cover the entire spinal cord using two overlapping slabs (Fig. 1). Reduced FOV DTI scan parameters were: number of directions = 20; b = 800 s/mm^2; voxel size = $0.8 \times 0.8 \times 6.0$ mm^3; matrix size = 36×208; axial slices = 40; repetition time TR = 7900 ms; echo time TE = 11 0ms; number of averages = 3; and acquisition time = 16.98 min (to collect both slabs). Cardiac gating and respiratory compensation were not used in this study because this would increase acquisition time, which is not desirable in pediatric imaging. Also, anesthesia was not administrated to the subjects in this study.

Pre-processing of diffusion tensor imaging data

Motion correction. Motion artifacts induced by patient movement, spinal cord pulsation and oscillation, and cardiac and respiratory motion can be reduced using sedation, cardiac gating, and respiratory compensation. Unfortunately, in pediatric imaging, these techniques increase scanning time, which may result in a lack of patience and cooperation by patients.[17,27–29] Although the implementation of the 2D RF diffusion sequence helped to mitigate image contamination attributed to these effects, motion correction was performed to further enhance tensor estimation accuracy.[17] Diffusion-weighted images were aligned with the average reference image (b0) using a rigid body registration algorithm and a normalized mutual information cost function using an in-house software developed in Matlab (The MathWorks, Inc., Natick, MA).[17,28–30]

Diffusion tensor estimation

After data acquisition and preprocessing, a robust estimation of tensor by outlier rejection (RESTORE) technique was applied to generate DTI maps, including fractional anisotropy (FA) and mean diffusivity (MD). This method uses iteratively reweighted least-squares regression to identify potential outliers and subsequently exclude them. The final fit is performed with the remaining data

Table 1. Demographic and Clinical Characteristics of the SCI Patients

Subject	*Age at the time of study*	*Age at the time of injury*	*Time after initial SCI*	*Level of injury-based ISNCSCI*	*Severity of injury-based AIS*
SCI1	9.25	1.75	7.50	C6	B
SCI2	15.18	12.33	2.85	T10	B
SCI3	10.01	4.00	6.01	C5	D
SCI4	11.14	4.75	6.39	C6	A
SCI5	15.16	12.00	3.16	L2	Unable to determine
SCI6	11.07	1.50	9.57	T4	A
SCI7	9.44	8.25	1.19	T9	A
SCI8	8.08	3.67	4.41	C1	D
SCI9	13.74	0.50	13.24	C5	D
SCI10	8.10	2.08	6.02	C8	A
SCI11	15.74	12.00	3.74	T9	A
SCI12	12.40	1.42	10.98	C1	D
SCI13	12.63	1.58	11.05	Unable to determine (thoracic SCI)	Unable to determine
SCI14	12.71	8.42	4.29	T12	A
SCI15	8.05	3.42	4.63	Unable to determine (thoracic SCI)	A
SCI16	8.68	0.67	8.01	Unable to determine (cervical SCI)	Unable to determine
SCI17	15.00	13.85	1.42	C8	A
SCI18	7.04	1.33	5.71	L2	D
SCI19	7.17	0 (at birth)	7.17	Unable to determine (thoracic SCI)	Unable to determine
SCI20	14.91	13.08	1.83	T4	D

SCI, spinal cord injury; ISNCSCI, International Standards for Neurological Classification of Spinal Cord Injury; AIS, American Spinal Injury Association Impairment Scale.

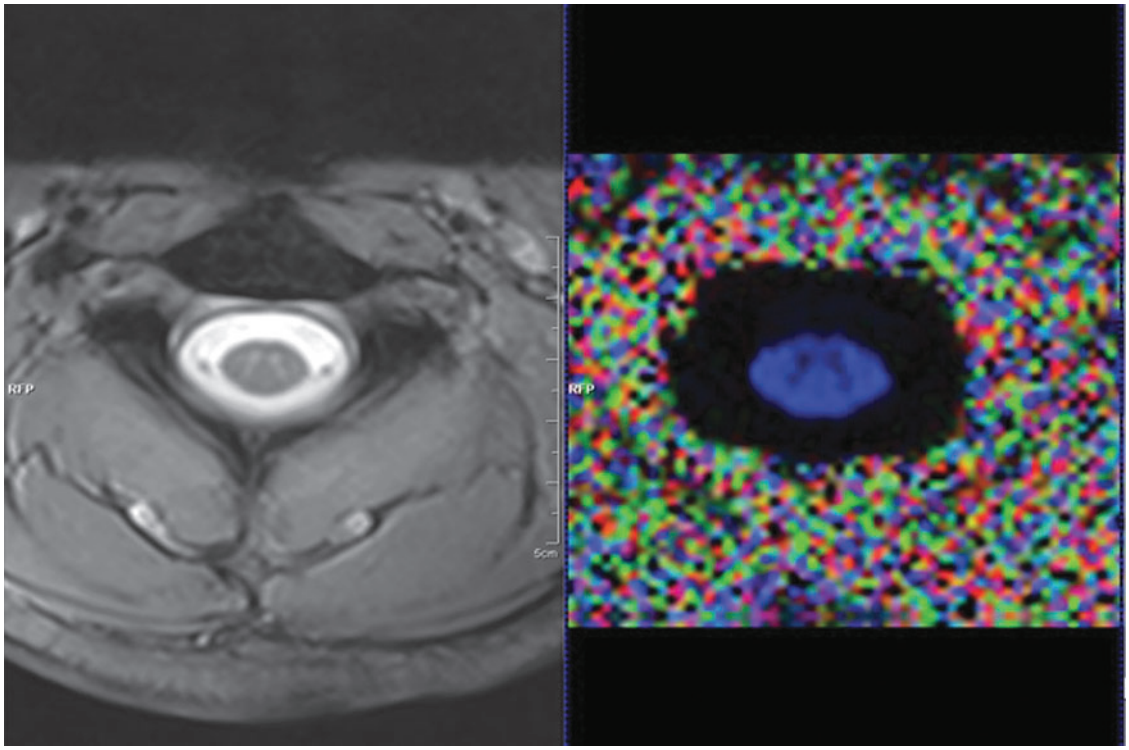

FIG. 1. Cross-sectional image of the spinal cord acquired from the MRI scanner; T2 W-GRE image (left) and FA map reconstructed from raw DTI dataset (right). DTI, diffusion tensor imaging; FA, fractional anisotropy; MRI, magnetic resonance imaging; T2 W-GRE, T2-weighted gradient recalled echo. Color image is available online at www.liebertpub.com/neu

points using the constant weights that appropriately describe the errors introduced by Gaussian distributed noise. This method eliminates the need for identifying corrupted images manually and automatically detects spatially localized outliers that would be easily missed by visual inspection.[31]

Generation of fiber tracts (tractography)

Fiber tracts were assigned for each seed (voxel) belonging to the WM of every slice to generate whole spinal cord tracts. A specific threshold was set to include WM and exclude CSF and GM (Fig. 2). These tracts were then restricted to the user defined regions of interest (ROIs) placed at each intervertebral disk level and at the mid-vertebral body level of the cervical and thoracic spinal cord (approximately 40 ROIs).

In this study, fiber tracts were generated for both TD and SCI subjects. It is known that GM and CSF have lower FA values than WM.[29] To construct only WM tracts, FA thresholds were set for both TD and SCI cases at 40–50% of the average FA value.[29] The streamline-based deterministic method traces pathways from a seed (voxel) by following the primary eigenvector from one voxel to the next by knowing the propagation direction, length, and step of each propagation. A tract is terminated when it reaches a voxel with FA values lower than a predefined threshold followed by estimation of the turning angle of the fiber orientation predefined by an angular threshold (e.g., 70 degrees).[29]

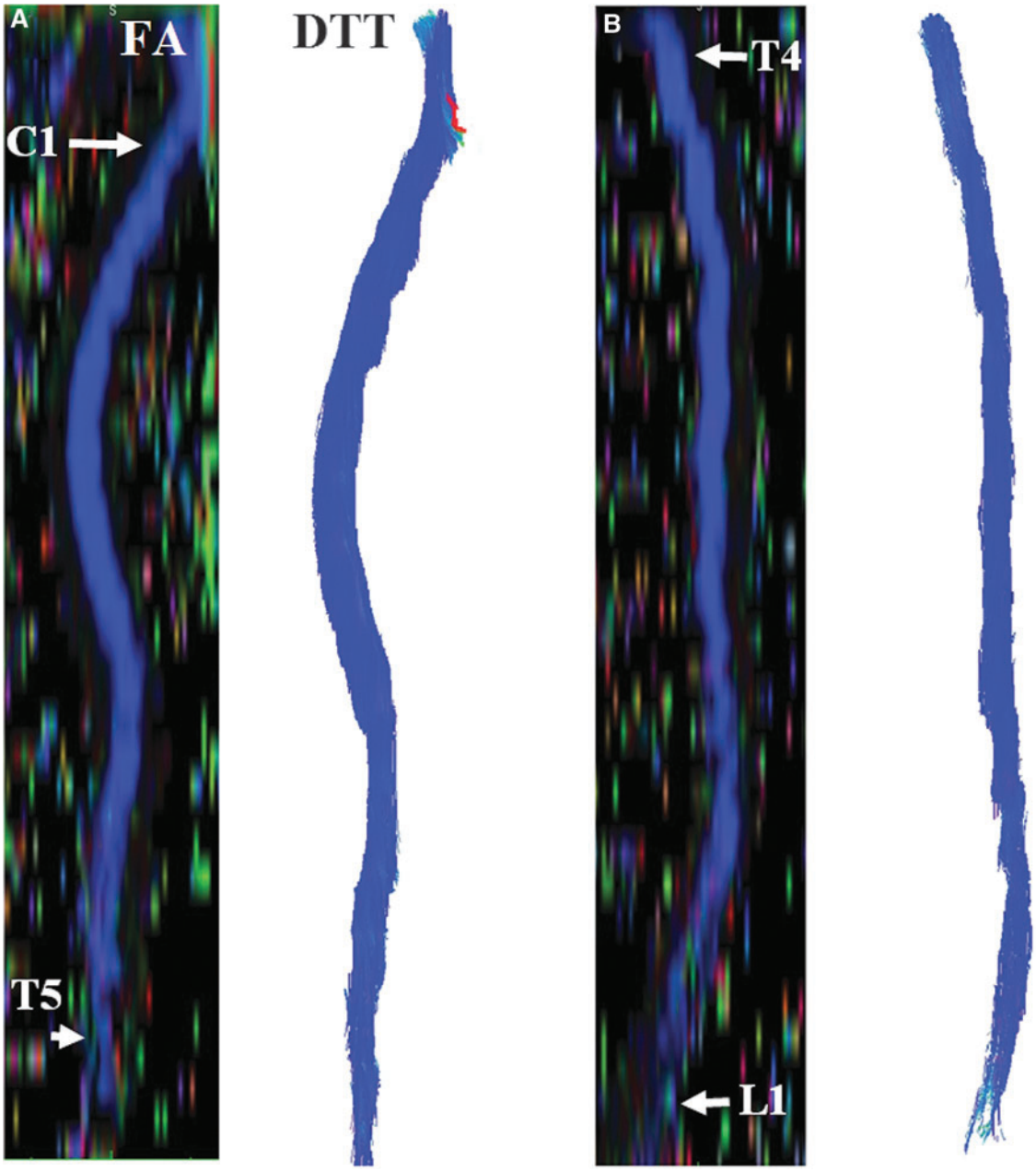

FIG. 2. Sagittal reconstruction of FA color maps of 2 overlapping slabs (**A** and **C**). The cervical and upper thoracic regions (A) and corresponding tractography image (**B**). The upper thoracic-through-conus regions (C) and corresponding tractography image (**D**). DTT, diffusion tensor tractography; FA, fractional anisotropy. Color image is available online at www.liebertpub.com/neu

Manual region of interest definition

To measure DTI and DTT at each intervertebral disk level and at the mid-vertebral body level of the cervical and thoracic spinal cord, ROIs were drawn manually on each FA map. These ROIs included both the GM and WM of the spinal cord and excluded the border, or edge, of the cord (approximately 1–2 voxels from outer margin of the cord) to avoid the effects of partial volume artifacts that occur at the cord/CSF interface (Fig. 3). This procedure was followed throughout at each intervertebral disk level and at the mid-vertebral body level of the cervical and thoracic spinal cord, being anatomically localized by an independent board-certified neuroradiologist, in all subjects. These levels are: C1, mid-dens, base dens, mid-C2, C2–C3, mid-C3 (upper cervical cord); C3–C4, mid-C4, C4–C5, mid-C5 (middle cervical cord); C5–C6, mid-C6, C6–C7, mid-C7, C7–T1 (lower cervical cord); mid-T1, T1–T2, mid-T2, T2–T3, mid-T3, T3–T4, mid-T4, T4–T5 (upper thoracic cord); mid-T5, T5–T6, mid-T6, T6–T7, mid-T7, T7–T8, mid-T8, T8–T9 (middle thoracic cord); mid-T9, T9–T10, mid-T10, T10–T11, mid-T11, T11–T12, mid-T12, T12–L1, mid-L1 (lower thoracic cord).

DTI and DTT measures were computed for all subjects in both the normal ($n=23$) and SCI ($n=20$) groups and averaged along ROIs drawn at each intervertebral disk level and at the mid-vertebral body level of the cervical and thoracic spinal cord (approximately 40 ROIs for each subject). Also, the proposed quantitative measures were calculated and compared with the TD subjects at the regions superior to the relative injury region in patients with thoracic SCI and inferior to the relative injury region in patients with cervical SCI. Figure 4 shows a representative above- and below-level breakdown for a subject with a chronic cervical injury. In cervical SCI ($n=10$), only the thoracic average (*which is the common region for all cervical SCI no matter where the level of injury is*) was compared with the thoracic average of the normal population ($n=23$). In the thoracic SCI group ($n=10$), the cervical area (*which is the common region for all thoracic SCI no matter where the level of injury is*) was compared with cervical average of the normal group (n = 23)

Statistical anlysis

Upon definition of whole-cord ROIs, statistical analysis was performed between subjects with SCI and TD control groups. A comprehensive data table was created containing information of DTI and DTT measures (Tables 2–4). Mean and SD of each measure for every subject along the entire spinal cord were calculated. These measures then were compared between TD and SCI subjects based on standard least squared linear regression model and restricted maximum likelihood method (JMP Pro 13.0 software). This model was constructed looking at group differences by assuming ROI level and groups (controls/patients) composition as the fixed effects and subjects as the random effects. The same statistical analysis was also performed when investigating diffusion changes above (for thoracic injuries) and below (for cervical injuries) between TD and SCI subjects.

A p value of 0.05 was used throughout to determine statistical significance.

Results

The mean FA values of the whole cord along the entirety of the spinal cord in the controls and patients were 0.46 ± 0.11 and 0.37 ± 0.09, respectively. FA values were significantly decreased in patients with SCI ($p < 0.0001$) when compared to controls. MD values in the controls and patients were $0.94 \pm 0.09 \times 10^{-3}$mm^2/sec and $1.01 \pm 0.08 \times 10^{-3}$mm^2/sec, respectively; however, it was not a statistically significant difference. Also, DTT parameters, such as mean length of tracts and tract density, were calculated using the streamline tractography algorithm. The mean tract density in the controls and patients were 405.93 ± 243.84 and 268.90 ± 270.34, respectively, which shows a significant decrease in the SCI group ($p = 0.0005$). However, the mean length of tracts (55.21 ± 30.18 and 43.28 ± 18.56 mm in the controls and patients, respectively) did not show significant differences (Table 2). Figure 5 represents these quantitative measures at various cord levels.

Also, DTI and DTT parameters were calculated above the injury site (cervical) in patients with thoracic SCI and below the injury site

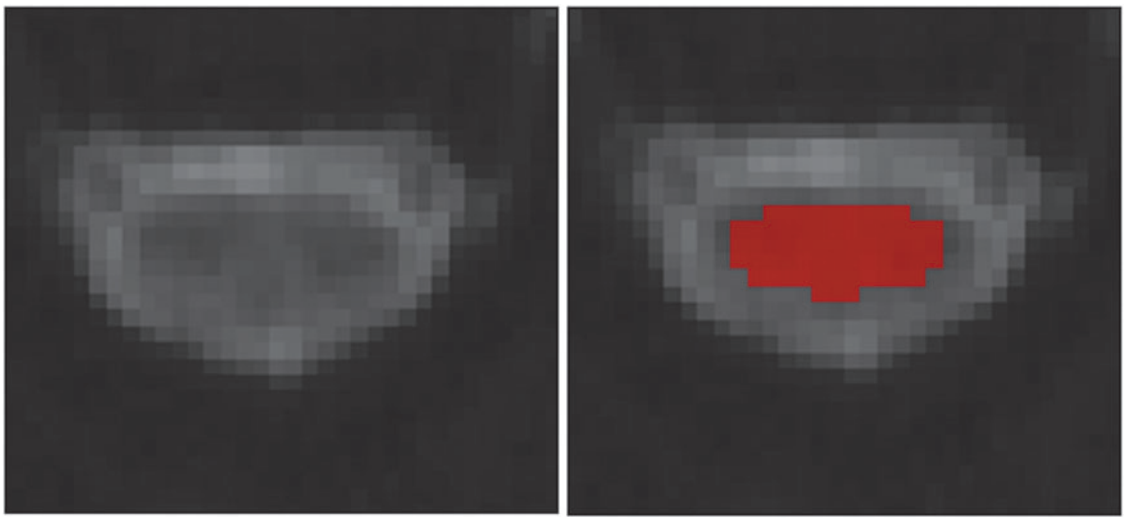

FIG. 3. Illustration of placement of ROIs on FA map after being anatomically localized by level by a board certified neuroradiologist. To avoid partial volume averaging with CSF, ROI was chosen away with a minimum of one voxel from the border or edge of the cord. CSF, cerebrospinal fluid; FA, fractional anisotropy; ROIs, regions of interest. Color image is available online at www.liebertpub.com/neu

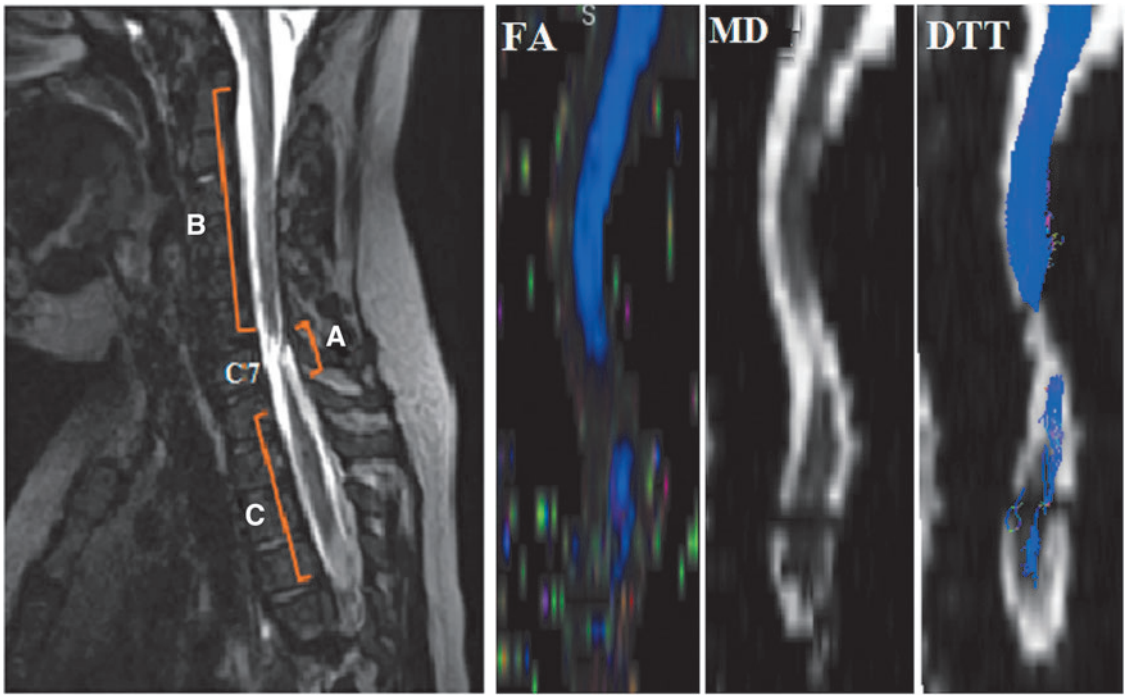

FIG. 4. Sagittal T2-weighted image of a representative subject with chronic traumatic injury in the cervical area (left) and FA, MD and tractography images created by DTI data (right). Three regions relative to injury: regions superior to injury epicenter (B), at injury epicenter (A), and inferior to injury epicenter (C) were identified. Injury epicenter for this subject located at C7 vertebral level. DTT, diffusion tensor tractography; FA, fractional anisotropy; MD, mean diffusivity. Color image is available online at www.liebertpub.com/neu

(thoracic) in patients with cervical SCI (Tables 3 and 4). In the patients with cervical SCI, a decrease in mean FA, WM tract density, and mean length of tracts and an increase in MD were observed below the injury levels (thoracic region). Statistically significant decreases have been shown in FA ($p < 0.0001$) and tract density ($p < 0.0001$). However, the mean length of tracts did not show significant differences.

DTI and DTT changes in the patients with thoracic SCI were similar to the cervical SCI group. Compared to TD, a decrease in mean FA, WM tract density, and mean length of tracts and an increase in MD were observed above the injury levels (cervical region). Statistically significant decreases were shown only in tract density above the injury ($p = 0.004$). FA, MD, and length of tracts did not show significant changes above the injury levels.

Discussion

DTT and DTI have been underexplored for the evaluation of the pediatric spinal cord because of the relatively small size of the spinal cord and the motion artifacts induced by CSF pulsation, cardiac, and respiration.[6,32] However, development of newer pulse sequence methods, such as reduced FOV, has enabled reliable DTI collection and enabled further exploration of the spinal cord. In this study, DTI and deterministic tractography were used to successfully examine pathological changes in SCI patients compared to TD controls. The results demonstrate that theses quantitative measures have potential to show the deformation and functional integrity of the cord at the level of injury and above or below. Also, tissue degeneration of the spinal cord above, below, and at the lesion can normally be detected by histological examination, but not by visual inspection of the image of the tissue. This work demonstrated that the

Table 2. Averaged DTI and DTT Quantitative Measures of the Whole Cord of Controls and Patients with SCI Along Entire Spinal Cord (Cervical and Thoracic)

Features	*TD* *Mean ± SD*	*SCI* *Mean ± SD*	*Prob>|t|*
FA	0.46 ± 0.11	0.37 ± 0.09	<0.0001
MD (10^{-3}mm^2/s)	0.94 ± 0.09	1.01 ± 0.08	0.12
Length of tracts (mm)	55.21 ± 30.18	43.28 ± 18.56	0.08
Tract density	405.93 ± 243.84	268.90 ± 270.34	<0.0001

DTI, diffusion tensor imaging; DTT, diffusion tensor tractography; SCI, spinal cord injury; FA, fractional anisotropy; MD, mean diffusivity; TD, typically developing; SD, standard deviation.

Table 3. Averaged DTI and DTT Parameters of the Whole Cord of Controls and Patients with Cervical SCI Along Entire Cervical Spinal Cord

Features	*TD* *Mean ± SD*	*BIR* *Mean ± SD*	*Prob>|t|*
FA	0.45 ± 0.12	0.34 ± 0.08	<0.0001
MD (10^{-3}mm^2/s)	0.86 ± 0.09	0.94 ± 0.07	0.2
Length of tracts (mm)	57.71 ± 6.58	42.02 ± 15.98	0.95
Tract density	323.76 ± 207.33	148.25 ± 100.51	<0.0001

DTI, diffusion tensor imaging; DTT, diffusion tensor tractography; SCI, spinal cord injury; FA, fractional anisotropy; MD, mean diffusivity; TD, typically developing; BIR, below injury region; SD, standard deviation.

Table 4. Averaged DTI and DTT Parameters of the Whole Cord of Controls and Patients with Thoracic SCI Along Entire Thoracic Spinal Cord

Features	*TD* *Mean ± SD*	*AIR* *Mean ± SD*	*Prob>|t|*
FA	0.47 ± 0.09	0.41 ± 0.11	0.62
MD (10^{-3}mm^2/s)	1.04 ± 0.08	1.1 ± 0.07	0.5
Length of tracts (mm)	51.67 ± 16.95	48.04 ± 23.9	0.6
Tract density	522.31 ± 244.57	497.24 ± 405.49	0.004

DTI, diffusion tensor imaging; DTT, diffusion tensor tractography; SCI, spinal cord injury; FA, fractional anisotropy; MD, mean diffusivity; TD, typically developing; AIR, above injury region; SD, standard deviation.

quantitative measurements offered by DTI and DTT might reveal functional changes associated with SCI away from the injury site.

Standard DTI parameters, such as FA and MD, have become common measures used to assess the integrity of the spinal cord. When comparing diffusion metrics between TD and subjects with SCI, studies have shown a decrease in FA and an increase in MD.[4,33] Our results are consistent with these findings; however, only FA was statistically significant. The decrease in FA may be indicative of Wallerian degeneration from the site of injury. Degeneration of the fiber architecture, specifically the myelin, will permit diffusion perpendicular to the neuronal axis, thus lowering the degree of FA.[26,33] Although not statistically significant, the increase in MD may be attributed to an increase in cord edema.[33]

In addition to DTI, DTT has become a supplementary method used to visualize and quantify the WM of the spinal cord. DTT offers a number of measures, including length of fiber tracts and tract density, which could provide insight into the condition of the cord after traumatic injuries. Past DTT studies have shown a decrease in tract density and no difference in mean tract length in subjects with cervical SCI compared to healthy subjects.[28] The techniques used in this study revealed similar results. The significant decrease in tract density provides additional insight into the degeneration process in chronic SCI cases. It is clear that degeneration not only occurs at the site of injury, but also the surrounding areas. A future study involving the comparison of adult fiber degeneration and pediatric fiber degeneration may elucidate differences in the processes the body undergoes at younger ages.

Generation of fiber tracts was achieved by the use of deterministic streamline tractography. Many studies have proven the effectiveness of this algorithm, providing evidence that the estimated trajectories of WM fiber tracts are indicative of cord conditions.[28] This method is rather quick and simple to calculate compared to other techniques. However, there are limitations, notably difficulty in interpreting the crossing of fiber tracts. Deterministic tractography relies on the assumption that a voxel contains one single orientation. The average diameter of a neuron is 0.1 mm. Using the voxel size of $0.8 \times 0.8 \times 6.0$ mm, it is certainly possible that a single voxel will contain numerous fibers that may not have the same orientations. Different tracts may cross within a single voxel; therefore, imprecise data may be obtained. An alternative to deterministic is probabilistic fiber tracking. Probabilistic fiber tracking is an algorithm that calculates a probability distribution of fiber orientations to estimate the likelihood of a tract. As a benefit, voxels that contain relatively low FA values, such as areas where fibers cross, will still be integrated into the tract.

The techniques performed revealed significant decreases in both FA and tract density in SCI subjects compared to TD subjects. This may be attributed to a number of factors. This study evaluated the changes in DTI and DTT measures of TD children ranging from ages 6 to 16 and children with SCI ranging from 7 to 16 years of age. Past studies have revealed age-related changes in diffusion tensor metrics as a result of natural maturation of the central nervous system (CNS), primarily myelination and axonal growth.[32] Thus, these significant changes observed may be skewed because of these age-related influences. By having a larger sample size, the analysis can be done as a function of age to minimize DTI and DTT variabilities attributed to maturation.

After the acquisition of axial DTI images, ROIs were manually drawn at each slice of the FA maps to isolate the WM from the GM. The use of ROIs as a direct measure has been proven to help understand specific areas of the CNS, such as neurodevelopmental

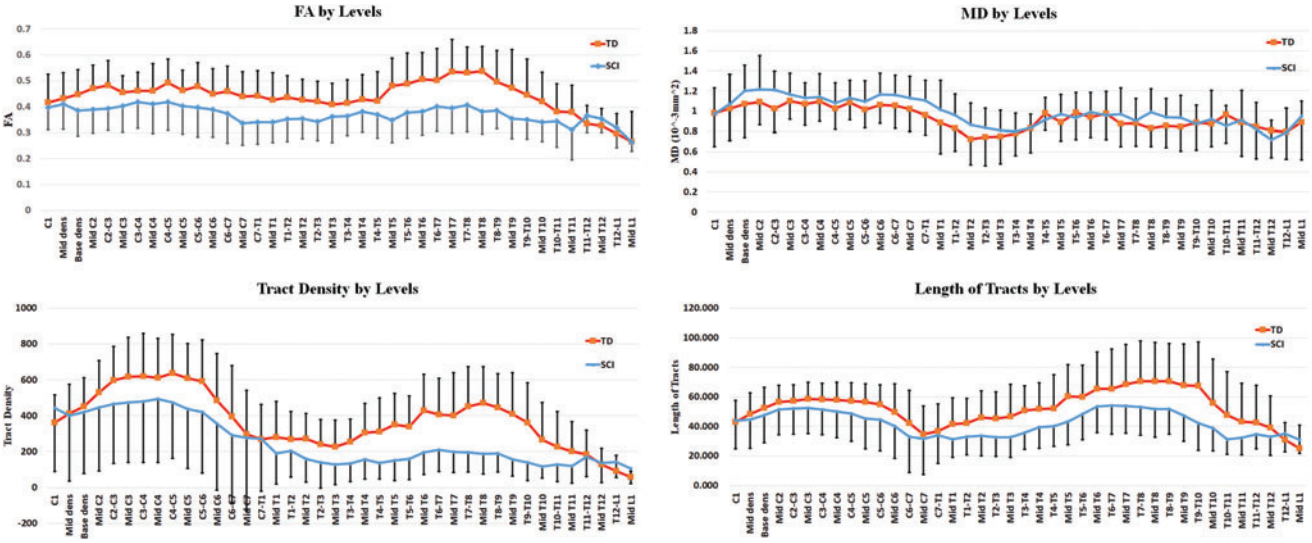

FIG. 5. Averaged DTI and DTT measures across all TD and SCI subjects and plotted as a function of cord levels. The error bars represent the standard deviations. DTI, diffusion tensor imaging; DTT, diffusion tensor tractography; SCI, spinal cord injury; TD, typically developing. Color image is available online at www.liebertpub.com/neu

changes. However, this method has limitations, including inter- and intrarater variability and the length of time that drawing requires. Hand drawing an ROI is subjective. Typically, the outer border of an ROI will be drawn 1–2 voxels from the edge of the cord. This ambiguous guideline leaves opportunity for bias from a researcher between slices and especially between one researcher and another, thus increasing variability of data. Additionally, it is time-consuming to draw an ROI at each slice, especially as the number of subjects increase. Therefore, there is need for an automated or semiautomated ROI delineation that is validated to be as accurate or more accurate than manually drawn ROIs.

It has been demonstrated in past studies that diffusion values are not uniform throughout the cord. Different levels of the cord will vary in width and diameter depending on the number of neural projections to the body and extremities. Variation in the volume of WM will thus change the values of DTI parameters.

Several human and animal studies have shown the relative importance of the cord above and below the level of injury in SCI patients.[35–37] With that goal, we decided to investigate the differences between DTI and DTT measures of the following groups: 1) between normal and SCI group; 2) in cervical SCI, only the thoracic slices (*which is the common region for all cervical SCI no matter where the level of injury is*) was compared with the thoracic average of the normal population; and 3) in the thoracic SCI group, the cervical area (*which is the common region for all thoracic SCI no matter where the level of injury is*) was compared with the cervical average of the normal group. Although our group results showed that in the cord above (in thoracic injury patients) and below (in cervical injury patients) there were statistically significant changes compared to the normal healthy controls, our sample size was small to deduce the utility of these findings to a single subject's treatment and rehabilitation status. Future studies with a larger sample size and with various ASIA categories are necessary to address this.

Conclusion

To quantitatively characterize both the functional and structural organization of the spinal cord is an advancement that could potentially aid in supporting diffusion imaging as a biomarker for SCI. With the emergence of diffusion and tractography techniques, we have entered an era in which we can reconstruct neuronal fibers of the cord and quantify the mechanism that actuates the delicate machinery of our CNS. Unfortunately, such complex structures are vulnerable to injury. In this study, the effectiveness of DTI and DTT of the cervical and thoracic pediatric spinal cord as indicators of abnormal spinal cord conditions were examined. When comparing TD and SCI subjects, significant changes to DTI and DTT parameters we observed. FA and tract density appear to be the most sensitive parameters in assessing the state of the spinal cord in pediatric chronic SCI. These DTI and DTT metrics have the potential to provide clinical benefit. Previous studies from our group evaluated the predictive validity of DTI by examining its diagnostic accuracy for pediatric cervical SCI.[2] Strong associations between FA and clinical and MRI findings were reported. It has been shown that FA has strongest overall predictor of each clinical end point among other DTI measures (MD, axial diffusivity, and radial diffusivity) in pediatric cervical SCI.[2] In the future, we plan to examine diagnostic accuracy of both DTI and DTT measures of entire pediatric SCI and further analyze the impact of DTI and DTT on clinical findings. Therefore, we conclude that both DTI and DTT have demonstrated to be potential imaging biomarkers in the identification of spinal cord aberrations in SCI patients.

Acknowledgments

This work was supported by National Institute of Neurological Disorders of the National Institutes of Health under award number R01NS079635.

Author Disclosure Statement

No competing financial interests exist.

References

1. Kirshblum, S.C., Burns, S.P., Sorensen, F.B., Donovan, W., Graves, D.E., Jha, A., Johansen, M., Jones, L., Krassioukov, A., Mulcahey, M.J., Schmidt-Read, M., and Waring, W. (2011). International standards for neurological classification of spinal cord injury. J. Spinal Cord Med. 34, 535–546.
2. Mulcahey, M.J., Samdani, A.F., Gaughan, J.P., Barakat, N., Faro, S., Shah, P., Betz, R.R., and Mohamed, F.B. (2013). Diagnostic accuracy of diffusion tensor imaging for pediatric cervical spinal cord injury. Spinal Cord 51, 532–537.
3. Mulcahey, M.J., Gaughan, J., Betz, R.R., and Johansen, K.J. (2007). The International standards for neurological classification of spinal cord injury: reliability of data when applied to children and youths. Spinal Cord 45, 452–459.
4. Renoux, J., Facon, D., Fillard, P., Huynh, I., Lasjaunias, P., and Ducreux, D. (2006). MR diffusion tensor imaging and fiber tracking in inflammatory diseases of the spinal cord. AJNR Am. J. Neuroradiol. 27, 1947–1951.
5. Mohamed, F.B., Hunter, L.N., Barakat, N., Liu, C.S., Sair, H., Samdani, A.F., Betz, R.R., Faro, S.H., Gaughan, J., and Mulcahey, M.J. (2011). Diffusion tensor imaging of the pediatric spinal cord at 1.5T: preliminary results. AJNR Am. J. Neuroradiol. 32, 339–345.
6. Beaulieu, C. (2002). The basis of anisotropic water diffusion in the nervous system—a technical review. NMR Biomed. 15, 435–455.
7. Fujiyoshi, K., Yamada, M., Nakamura, M., Yamane, J., Katoh, H., Kitamura, K., Kawai, K., Okada, S., Momoshima, S., Toyama, Y., and Okano, H. (2007). In vivo tracing of neural tracts in the intact and injured spinal cord of marmosets by diffusion tensor tractography. J. Neurosci. 27, 11991–11998.
8. Fujiyoshi, K., Konomi, T., Yamada, M., Hikishima, K., Tsuji, O., Komaki, Y., Momoshima, S., Toyama, Y., Nakamura, M., and Okano, H. (2013). Diffusion tensor imaging and tractography of the spinal cord: from experimental studies to clinical application. Exp. Neurol. 242, 74–82.
9. Alexander, A.L., Lee, J.E., and Aaron, F.S. (2007). Diffusion tensor imaging of the brain. Neurotherapeutics 4, 316–329.
10. Madden, D.J., Bennett, I.J., Burzynska, A., Potter, G.G., Chen, N.K., and Song, A.W. (2012). Diffusion tensor imaging of cerebral white matter integrity in cognitive aging. Biochim. Biophys. Acta. 1822, 386–400.
11. Basser, P.J., and Jones, D.K. (2002). Diffusion-tensor MRI: theory, experimental design and data analysis—a technical review. NMR Biomed. 15, 456–467.
12. Maier, S.E., and Mamata, H. (2005). Diffusion tensor imaging of the spinal cord. Ann. N. Y. Acad. Sci. 1064, 50–60.
13. Ducreux, D., Lepeintre, J.F., Fillard, P., Loureiro, C., Tadie, M., and Lasjaunias, P. (2006). MR diffusion tensor imaging and fiber tracking in 5 spinal cord astrocytomas. AJNR Am. J. Neuroradiol. 27, 214–216.
14. Facon, D., Ozanne, A., Fillard, P., Lepeintre, J., Tournoux-Facon, C., and Ducreux, D. (2005). MR diffusion tensor imaging and fiber tracking in spinal cord compression. AJNR Am. J. Neuroradiol. 26, 1587–1594.
15. Tsuchiya, K., Fujikawa, A., and Suzuki, Y. (2005). Diffusion tractography of the cervical spinal cord by using parallel imaging. AJNR Am. J. Neuroradiol. 26, 398–400.
16. Finsterbusch, J. (2009). High-resolution diffusion tensor maging with inner field-of-view EPI. J. Magn. Reson. Imaging 29, 987–993.
17. Middleton, D.M., Mohamed, F.B., Barakat, N., Hunter, L.N., Shellikeri, S., Finsterbusch, J., Faro, S.H., Shah, P., Samdani, A.F., and Mulcahey, M.J. (2014). An investigation of motion correction algorithms for pediatric spinal cord DTI in healthy subjects and patients with spinal cord injury. Magn. Reson. Imaging 32, 433–439.

18. Cruz, L.C., Jr., Domingues, R.C., and Gasparetto, E.L. (2009). Diffusion tensor imaging of the cervical spinal cord of patients with relapsing-remising multiple sclerosis: a study of 41 cases. Arq. Neuropsiquiatr. 67, 391–395.
19. Setzer, M., Murtagh, R.D., Murtagh, F.R., Eleraky, M., Jain, S., Marquardt, G., Seifert, V., and Vrionis, F.D. (2010). Diffusion tensor imaging tractography in patients with intramedullary tumors: comparison with intraoperative findings and value for prediction of tumor resectability. J. Neurosurg. Spine 13, 371–380.
20. Ozanne, A., Krings, T., Facon, D., Fillard, P., Dumas, J.L., Alvarez, H., Ducreux, D., and Lasjaunias, P. (2007). MR diffusion tensor imaging and fiber tracking in spinal cord arteriovenous malformations: a preliminary study. AJNR Am. J. Neuroradiol. 28, 1271–1279.
21. Rajasekaran, S., Kanna, R.M., Karunanithi, R., and Shetty, A.P. (2010). Diffusion tensor tractography demonstration of partially injured spinal cord tracts in a patient with posttraumatic brown sequard syndrome. J. Magn. Reson. Imaging 32, 978–981.
22. Somers, MF. (2009). *Spinal Cord Injury: Functional Rehabilitation*, 3rd ed. Pearson Education: Upper Saddle River, NJ.
23. Chang, Y., Jung, T.D., Yoo, D.S., and Hyun, J.K. (2010). Diffusion tensor imaging and fiber tractography of patients with cervical spinal cord injury. J. Neurotrauma 27, 2033–2040.
24. Lootus, M., and Church, C. (2015). Automated radiological analysis of spinal MRI. University of Oxford: Oxford, UK.
25. Mohamed, F.B., Hunter, L.N., Barakat, N., Liu, C.S., Sair, H., Samdani, A.F., Betz, R.R., Faro, S.H., Gaughan, J., and Mulcahey, M.J. (2011). Diffusion tensor imaging of the pediatric spinal cord at 1.5T: preliminary results. AJNR Am. J. Neuroradiol. 32, 339–345.
26. Barakat, N., Mohamed, F.B., Hunter, L.N., Shah, P., Faro, S.H., Samdani, A.F., Finsterbusch, J., Betz, R., Gaughan, J., and Mulcahey, M.J. (2012). Diffusion tensor imaging of the normal pediatric spinal cord using an inner field of view echo-planar imaging sequence. AJNR Am. J. Neuroradiol. 33, 1127–1133.
27. Conklin, C.J., Middleton, D.M., Alizadeh, M., Finsterbusch, J., Raunig, D.L., Faro, S.H., Shah, P., Krisa, L., Sinko, R., Delalic, J.Z., Mulcahey, M.J., and Mohamed, F.B. (2016). Spatially selective 2D RF inner field of view (iFOV) diffusion kurtosis imaging (DKI) of the pediatric spinal cord. Neuroimage Clin. 11, 61–67.
28. Figley, C.R., and Stroman, P.W. (2007). Investigation of human cervical and upper thoracic spinal cord motion: implications for imaging spinal cord structure and function. Magn. Reson. Med. 58, 185–189.
29. Alizadeh, M., Intintolo, A., Middleton, D.M., Conklin, C.J., Faro, S.H., Mulcahey, M.J., and Mohamed, F.B. (2016). Reduced FOV diffusion tensor MR imaging and fiber tractography of the pediatric cervical spinal cord. Spinal Cord 55, 314–320.
30. Barakat, N., Mohamed, F.B., Hunter, L.N., Shah, P., Faro, S.H., Samdani, A.F., Finsterbusch, J., Betz, R., Gaughan, J., and Mulcahey, M.J. (2012). Diffusion tensor imaging of the normal pediatric spinal cord Using an inner field of view echo planar imaging sequence. AJNR Am. J. Neuroradiol. 33, 1127–1133.
31. Chang, L.C., Jones, D.K., and Pierpaoli, C. (2005). RESTORE: robust estimation of tensors by outlier rejection. Magn. Reson. Med. 53, 1088–1095.
32. Xiuming, Z. (2015). A tutorial on restricted maximum likelihood estimation in linear regression and linear mixed-effects model. A*STAR-NUS Clinical Imaging Research Center. Available at: http://people.csail.mit.edu/xiuming/docs/tutorials/ReML.pdf. Accessed November 20, 2017.
33. Alizadeh, M., Mohamed, F.B., Faro, S.H., Shah, P., Conklin, C.J., Middleton, D.M., Saksena, S., Shahrampour, S., and Mulcahey, M.J. (2015). Intensity inhomogeneity correction in clinical pediatric spinal cord MRI images. Presented at the 41st annual Northeast Bioengineering Conference (NEBEC), Troy, NY, pps. 1–2.
34. Saksena, S., Middleton, D.M., Krisa, L., Shah, P., Faro, S.H., Sinko, R., Gaughan, J., Finsterbusch, J., Mulcahey, M.J., and Mohamed, F.B. (2016) Diffusion tensor imaging of the normal cervical and thoracic pediatric spinal cord. AJNR Am. J. Neuroradiol. 37, 2150–2157.
35. Choe, A.S., Sadowsky, C.L., Smith, S.A., Van Zijl, P.C., Pekar, J.J., and Belegu, V. (2017). Subject-specific regional measures of water diffusion are associated with impairment in chronic spinal cord injury. Neuroradiology 59, 747–758.
36. Jirjis, M.B., Kurpad, S.N., and Schmit, B.D. (2013). Ex vivo diffusion tensor imaging of spinal cord injury in rats of varying degrees of severity. J. Neurotrauma 30, 1577–1586.
37. Freund, P., Curt, A., Friston, K., and Thompson, A. (2012). Tracking changes following spinal cord injury: insights from neuroimaging. Neuroscientist 19, 116–128.

Address correspondence to:
Feroze B. Mohamed, PhD
Department of Radiology
Jefferson Integrated Magnetic Resonance Imaging Center
Thomas Jefferson University
909 Walnut Street
Philadelphia, PA 19107

E-mail: feroze.mohamed@jefferson.edu